Interplanar potentials derived from transverse oscillations of 3.5-MeV/amu He and Li nuclei in planar channels of silicon

C. D. Moak, J. Gomez del Campo, J. A. Biggerstaff, S. Datz,
P. F. Dittner, H. F. Krause, and P. D. Miller
Oak Ridge National Laboratory, Oak Ridge, Tennessee 37830
(Received 8 June 1981)

Transverse oscillations of ions moving in the planar channels of a crystal give information about their stopping powers versus amplitude of oscillation and about the restoring forces operating on the ions. In a previous paper M. T. Robinson has analyzed data on 3-MeV α particles, 10-MeV oxygen ions, and 15–60-MeV iodine ions in crystals of Au; at these energies the effective charges of the ions were unknown and had to be inferred by analysis of the channeling data. In this study we have used light ions at high enough energy to assure that each ion is a bare nucleus. Ions of ^{3}He, ^{4}He, ^{6}Li, and ^{7}Li at 3.5 MeV/amu have been used to give both a change of charge and change of charge-to-mass ratio. Robinson's analysis has been recast since, in this case, the ions' effective charges are known. A new procedure has been utilized to examine how well various approximations for interplanar potentials can be made to fit the data.

I. INTRODUCTION

Since most particles moving in planar channels of a crystal do not enter the crystal along the midplane, they generally oscillate transversely about the midplane between two sheets of atoms. Correlated small-angle scatterings cause the ions to return to (and cross) the midplane, executing transverse oscillations as shown in Fig. 1. If the beam of particles and the detector are aligned and well collimated, the detector will pick out groups of the trajectories which return the particles to the beam axis. Particles which do not have an integral number of oscillations will not be detected because their emergence angles will not coincide with that of the detector. For very small oscillation amplitudes, the particles will be able to reach the detector even if they have a nonintegral number of transverse oscillations because all emergence angles for those amplitudes are within the detector acceptance angle. Smaller amplitudes can be selectively studied by gradually reducing the detector acceptance angle. Near the center of the channel the interplanar potential is such that the oscillation frequencies become constant. In the harmonic region the frequency remains constant but the stopping power continues to fall very gradually to the minimum value which occurs at zero oscillation amplitude. Particles with larger amplitudes will have larger stopping powers since they travel in regions of greater electron density. The wavelength becomes

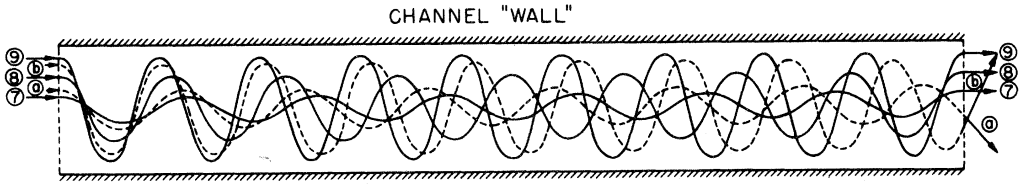

1. DETECTOR ALIGNED TO BEAM AXIS.
2. PATHS (7) (8) AND (9) EMERGE WITH DIRECTION UNCHANGED.
3. PATHS SUCH AS (a) AND (b) EMERGE WITH ALTERED DIRECTION.
4. AN IDENTICAL SET OF PATHS (OMITTED HERE) EXISTS FOR ENTRY BELOW MID-CHANNEL.
5. $(\Delta E)_9 > (E\Delta)_8 > (\Delta E)_7$ etc.
   $(\Delta E)_a$ AND $(\Delta E)_b$ ARE UNOBSERVED.
6. FOR THE CASE DRAWN HERE λ DECREASES WITH INCREASING OSCILLATION AMPLITUDE.

FIG. 1. Selection of energy loss groups according to angle of emergence of channeled particles.

 ©1982 The American Physical Society

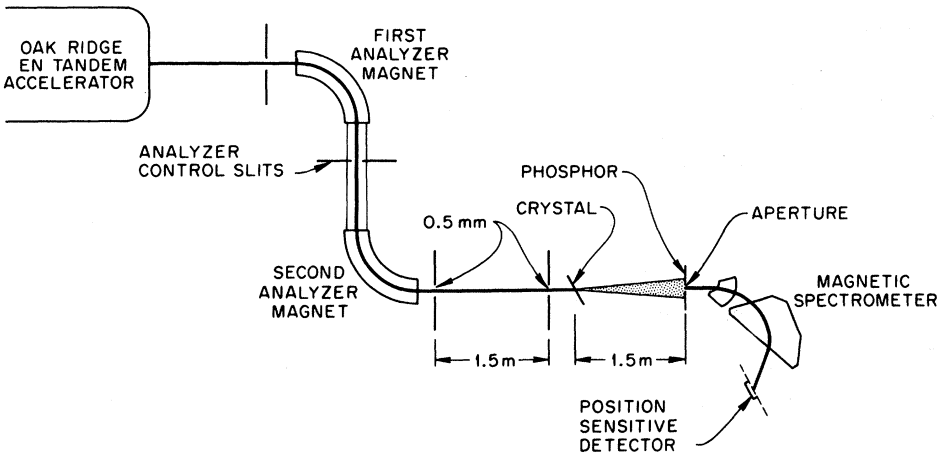

FIG. 2. Experimental arrangement.

shorter for larger amplitude so that wavelength, oscillation amplitude, and average stopping power are related. They are governed by the details of the restoring field. These effects cause the energy-loss spectrum to have a series of peaks, each peak corresponding to an integral number of wavelengths. If the crystal is tipped slightly, each trajectory will start at a different point on the wave and very small oscillation amplitudes will be eliminated. Further tipping eliminates more small amplitudes of oscillation and will accentuate the larger-amplitude, short-wavelength, large-stopping-power, groups. If the crystal is rotated about an axis perpendicular to the planes, the path length in the crystal will be increased and the geometry will select a series of longer wavelengths with smaller stopping powers.[1] Crystal rotation can give enough path-length variation to bring a given group with one oscillation number to the same stopping power as had been obtained previously for the adjacent group and thus one can map out the stopping power versus wavelength continuously over a wide range of oscillation amplitudes. Since the particles slow down along their paths the wavelengths are gradually shortened due to their reduced longitudinal velocity and some correction must be made for this effect. Robinson has developed a set of computer programs to derive oscillation frequencies from the data and analyze these in terms of interplanar potentials.[2]

II. EXPERIMENTAL ARRANGEMENT

The purpose was to measure channeling-group stopping powers under nearly identical conditions for ions of $^3He^{2+}$, $^4He^{2+}$, $^6Li^{3+}$, and $^7Li^{3+}$. The arrangement shown in Fig. 2 was used to provide collimation limits of $\sim 0.05°$ both for the incident beams and for the accepted portion of the emergent channeling patterns. Beams were extracted from the ORNL EN-tandem accelerator at energies of 3.5 MeV/amu, and the emergent channeled ions were momentum analyzed in an Enge split-pole magnetic spectrograph, equipped with a solid-state position-sensitive detector placed in the focal plane. The overall energy resolution of the beam and detection system was $\sim 0.4\%$. The target was a silicon crystal of 8.87 ± 0.13-μm thickness. During the course of the experiments, many values of the random energy loss for α particles were obtained. Values for random energy loss in Si have been given by Sellers, Hanson, and Kelley,[3] and these have been used to derive the thickness of the crystal used in the present experiments. To obtain emphasis upon various groups, the crystal was tipped slightly and then rotated to obtain a thickness variation of more than 50%. A typical energy spectrum is shown in Fig. 3 for the case of $^4He^{2+}$ ions at 3.5 MeV/amu channeled along the (111) plane in silicon.

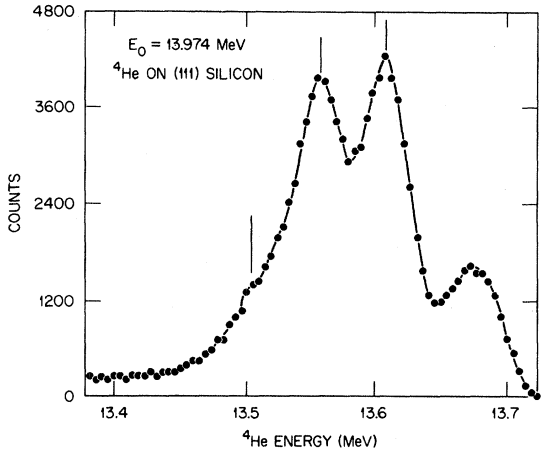

FIG. 3. Energy-loss groups; ^4He ions in (111) planar channels of Si.

III. EXPERIMENTAL RESULTS

The data were arranged for analysis in terms of energy loss versus effective thickness; to extract this information, it is necessary to follow the behavior of the energy spectra as the crystal thickness is changed by rotation about an axis perpendicular to the planes. Figure 4 shows an example for the case of ^{4}He ions at three different thicknesses, (9.76, 9.98, and 10.20 μm), where the number of counts are plotted against the energy loss $\Delta E/\Delta X$ in MeV/μm. The typical behavior (decreasing energy loss with increasing thickness) of the various groups (n) is illustrated by the shifts of the vertical lines. Energy loss data extracted from the peaks of the energy spectra, such as those shown in Fig. 4, are plotted against the effective thickness ΔX in the lower part of Fig. 5. The minimum energy loss, corresponding to particles of zero transverse amplitude was obtained by extrapolating the right-hand edges of the A_0 group for many different data runs (see Fig. 4). The centroid of the A_0 group is the average energy loss for all particles in the so-called harmonic region which extends out to 0.2 Å each side of the channel midplane. The position of this centroid is dependent upon the detector acceptance angle (but not the crystal mosaic spread[1]) and is therefore not a parameter used in the data analysis. The data in the lower part of Fig. 5 cover a range of transverse amplitudes from 0.2 to ~0.6 Å in the (110) channel; the half-width of the channel is 0.96 Å. The $\Delta E/\Delta X$ values illustrated are for ^{6}Li channeled along the (110) planes. Each oscillatory group (n) in Fig. 5 is characterized by decreasing energy loss for increasing thickness (solid lines on Fig. 5), and for each data point a value of the initial stopping power $(-dE/dX)_{E=E_0}$ and oscillatory frequency ω were obtained.[1] For the high velocity range of this experiment, the value of the stopping power exponent[1] is $p=-1$. The resulting values of the initial stopping powers and frequencies ω are plotted on the upper part of Fig. 5, using two different starting wave numbers 23 and 24 for Figs. 5(a) and 5(b), respectively. A least-squares fitting procedure was used to determine the value of n_0 which produced the best fit to all the data. This is illustrated in Figs.

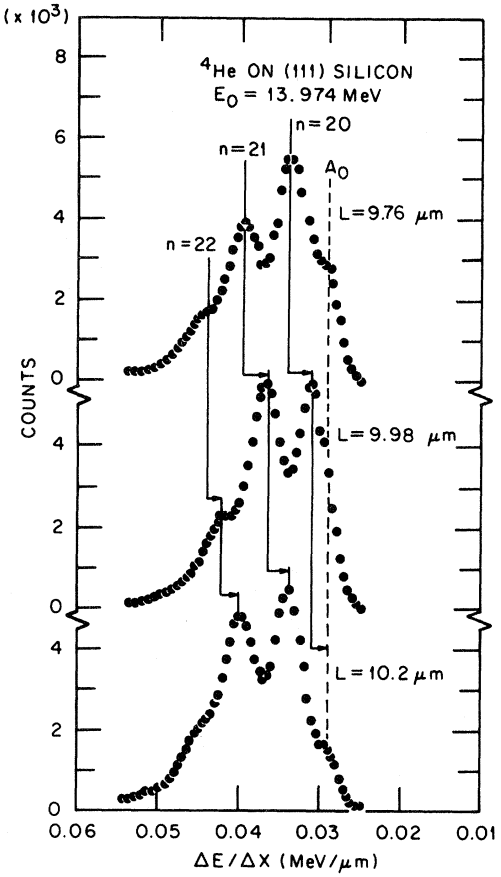

FIG. 4. Shifts of planar channel energy-loss groups vs crystal thickness.

TABLE I. Slopes, intercepts, and curvatures derived from the data.

Ion	$\alpha \pm \Delta\alpha$ (eV/Å)	$\beta \pm \Delta\beta$ (eV$^{1/2}$)	$s_0 \pm \Delta s_0$ (eV/Å)	$y \pm \Delta y$ (eV/Å^3)
		Experimental values for (110)		
^{3}He	−8.49 ±0.32	6.34 ±0.16	3.65 ±0.03	75.4 ±5.6
^{4}He	−9.69 ±0.28	7.12 ±0.14	3.59 ±0.03	71.6 ±4.2
^{6}Li	−21.58 ±0.34	13.01 ±0.14	8.35 ±0.08	108.8 ±3.4
^{7}Li	−22.75 ±0.38	13.50 ±0.15	8.00 ±0.08	106.8 ±3.6
		Experimental values for (111)		
^{3}He	−7.68 ±0.22	6.94 ±0.14	2.68 ±0.03	37.5 ±2.2
^{4}He	−7.14 ±0.23	6.86 ±0.15	2.74 ±0.03	34.9 ±2.1
^{6}Li	−16.94 ±0.22	12.60 ±0.11	6.36 ±0.06	55.6 ±2.2
^{7}Li	−16.60 ±0.21	12.40 ±0.10	5.96 ±0.06	55.5 ±2.1

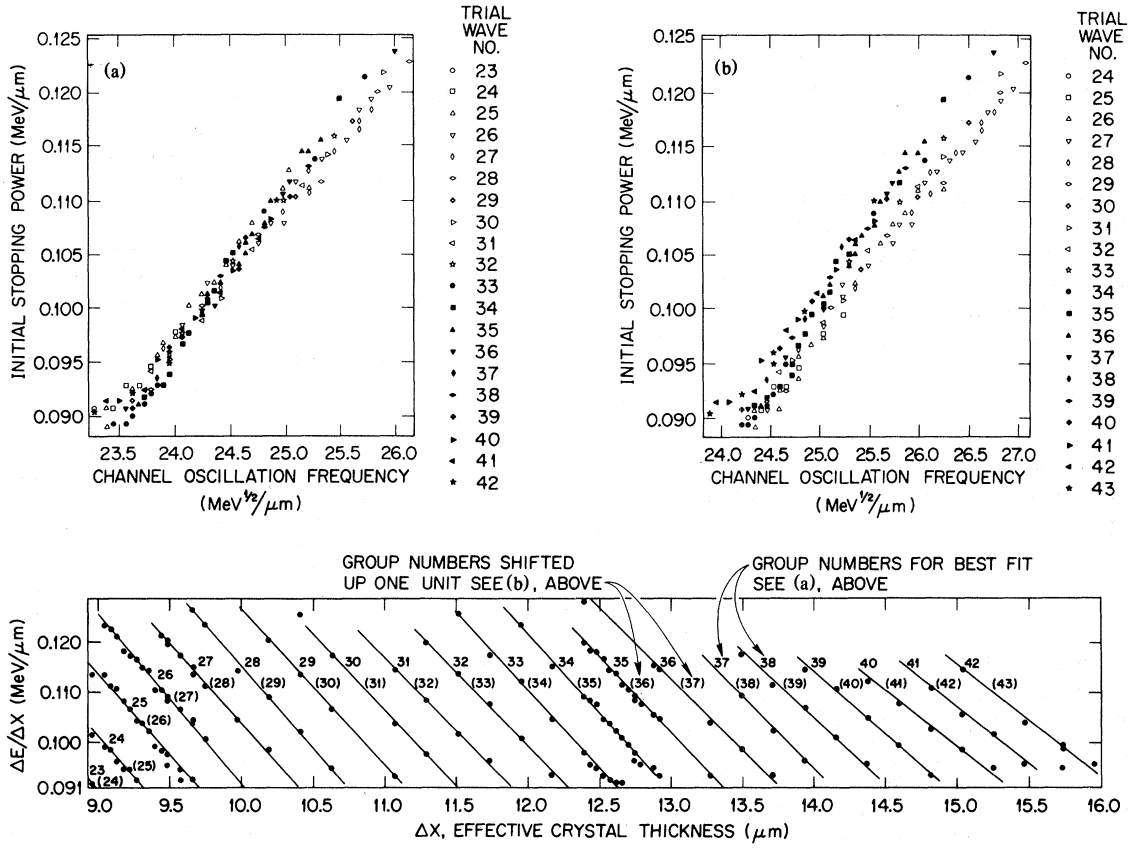

FIG. 5. Stopping power vs planar channel thickness, 21 MeV ^{6}Li in (100) channel of Si. (a) Oscillation frequency vs stopping power for trial first wave number 23. (b) Oscillation frequency vs stopping power for trial first wave number 24.

5(a) and 5(b), which displays the values of the initial stopping power versus ω for the best fit $n_0=23$ (a) and for a value of n_0 increased by one unit (b). A similar deterioration of fit occurs if n_0 is decreased by one unit. The linear relationship between $(-dE/dX)_{E=E_0}$ and ω can be written

$$\left(\frac{-dE}{dX}\right)_{E=E_0}=\alpha+\beta\omega \tag{1}$$

where α and β are the coefficients derived from the least-squares fit.[1,2] Table I shows the results for the α and β coefficients and the respective uncertainties. Also in Table I the stopping powers of the best channeled particles (leading edge values) s_0 are given. An important parameter in the analysis is the curvature (y) of the planar potential, which is defined by

$$y=2\pi^2(s_0-\alpha)^2/\beta^2 l \ , \tag{2}$$

where l is the half-width of the channel. The values of l are 0.96 and 1.1757 Å for the (110) and (111) planes, respectively. The extracted values of y from the experimental data are given in the last column of Table I.

The units of ω are such that a factor $M^{1/2}$ is suppressed. If two real oscillation frequencies (units t^{-1}) differ by the factor $(M_a/M_b)^{1/2}$, then in the absence of any isotope effect the values of ω would be the same. We expect that the values of α, β, s_0, and y should be the same for two isotopes. Errors in the value of the intercept α have a very small influence upon the value of the slope β derived from the data. The values of α for ^{3}He and ^{4}He lie outside their error values, especially for the (110) channel data; the discrepancy does not significantly alter the agreements between the values of s_0 and y. Except for this disagreement the data seem to prove that there is no isotope effect when comparing the results for ^{3}He and ^{4}He and for ^{6}Li and ^{7}Li.

IV. ANALYSIS OF THE PLANAR CHANNELING DATA

The motion of the ions passing between a pair of planes is decribed by the planar potential $V_2(X)$ given by

$$V_2(x)=V_1(l+x)+V_1(l-x) \ , \tag{3}$$

where x is the displacement from the center of the

channel and l is the half-width of the planar channel. $V_1(\bar{x})$ represents the interaction of the ions with the planar continuum potential given by

$$V_1(\bar{x}) = 4\pi\rho\kappa l \int_{\bar{x}}^{\infty} rV(r)\,dr \ , \tag{4}$$

where $V(r)$ is the interaction potential between the ion and a lattice atom separated by the distance r. The atomic density of the crystal is ρ; κ is a factor that accounts for the possibility of having parallel planes with different spacings. The factor κ is 1 for the (110) planar channels and $\frac{2}{3}$ for the (111) planar channels in Si.

Comparison of Eqs. (3) and (4) to the data can be made through the use of the curvature parameter y and the random stopping power $\hat{s}$. Equations for y and $\hat{s}$ in terms of the planar potential were derived by Robinson[2] and they are

$$y = V_2''(0)/l \ , \tag{5}$$

$$\hat{s} = \alpha + (\beta/\pi l)[V_2(l) - V_2(0)]^{1/2} \ . \tag{6}$$

Calculations of the curvature parameter y can be made with Eq. (5) for a given choice of the interaction potential $V(r)$, and comparisons can be made directly to the experimental y values deduced from the energy-loss measurements. From inspection of Eq. (6) we note that we can define a factor $\sigma' = (\hat{s} - \alpha)\pi/\beta$ (determined experimentally) which is a function only of the planar potential, i.e.,

$$\sigma' = [V_2(l) - V_2(0)]^{1/2}/l \ . \tag{7}$$

Previous analysis[1,2] using Eqs. (5) and (6) had the basic objective of extracting the planar potential from the experimental data and comparing this with the theory for a potential function of the Molière or Hartree-Fock type. The extraction of the interaction potential could be made only by comparing the ratios of the experimental y values of two different channels. This procedure cancels out the factor Z_1Z_2 appearing in $V(r)$, since Z_1Z_2 (the product of the effective charge states) is usually not known in channeling experiments with low velocity ions. In the present work for 3.5 MeV/amu He and Li ions, the energy is high enough to insure that the charge is the (totally stripped) nuclear charge. Using the Molière and Hartree-Fock potentials[2] and calculating the ratio of the y values for the (111) and (110) planes, the extracted inverse screening lengths (b) are 2.14 ± 0.26 and 1.95 ± 0.13 Å^{-1} for He and Li, respectively, for the Molière potential; for the Hartree-Fock potential, the values are 2.17 ± 0.26 Å^{-1} for He and 2.00 ± 0.13 Å^{-1} for Li. If we are to reproduce the absolute values of y, it would be necessary to arbitrarily normalize the Molière potential by a factor of 1.4 and the Hartree-Fock by 1.02. In Robinson's analysis of earlier data,[2] similar normalization factors were used for the Molière potential; however, for that case of channeling of low velocity ions, these factors were incorporated into uncertainties in Z_1, the effective charge, and therefore an independent check on the potential could not be made. In the present work for 3.5 MeV/amu He and Li ions, Z_1 is the bare nuclear charge and therefore the normalization factors must be related to the potential alone, and we conclude that the Molière potential has to be normalized by a large factor. This factor, if used in a low velocity regime, would predict unrealistically high effective charge states for He and Li. It should be noted that the inverse screening lengths b show an apparent decrease from He to Li (9.5% for the Molière and 8.5% for the Hartree-Fock potentials), but in both cases the differences are within our experimental uncertainty. A better way to test the adequacy of our analysis is to use a potential with no adjustable parameters, and this is achieved by using the $V(r)$ for the Hartree-Fock potential.[4]

For the case of channeling in the Si (111) planes, Eq. (3) had to be modified since this channel is bordered by pairs of closely spaced planes. The modification is[2]

$$V_2(x) = V_1(1+x) + V_1(l-x) + V_1(\tfrac{5}{3}l + x) + V_1(\tfrac{5}{3}l - x) \ , \tag{8}$$

where l is the half-width of the larger planar spacing (1.1757 Å).

Table II shows comparison between the experimental y values for He and Li (averaged over mass) and the predictions of Eq. (3) using the Hartree-Fock potential. The comparisons are shown for both planar channels, (110) and (111), and the agreement is excellent for the (110) planes and consistent with the experimental uncertainties for the (111) planes.

Table III shows the comparisons for the σ' factors. The column labeled σ'(theor)[b] corresponds to the calculated values without thermal corrections, and as can be seen they exceed the experimental values by about 2% for He (110), by about 4% for Li(110), and 18% for He and Li in (111). These discrepancies can be interpreted as due to effects of thermal vibrations of the atoms in the lattice. An approximate method to account for such effects is given as follows: Equa-

TABLE II. Comparisons between the experimental and theoretical curvature parameters y.

Ion	y_{110}(expt)	y_{110}(theor)	y_{111}(expt)	y_{111}(theor)
He	73.5 ±4.9	70.0	36.2 ±2.1	33.2
Li	107.8 ±3.5	105.0	55.5 ±2.2	49.5

tion (4) can be rewritten[5]

$$V_1(\bar{x}) = 4\pi\rho\kappa l \int_0^\infty rV(r)\,dr \int_{\bar{x}-r}^{\bar{x}+r} P(u)\,du \quad . \quad (9)$$

In Eq. (9) u is the thermal displacement perpendicular to the plane and $P(u)$ is a Gaussian distribution given by

$$P(u) = (2\pi\langle u^2\rangle)^{-1/2}\exp[-u^2(2\langle u^2\rangle)^{-1}] \quad , \quad (10)$$

where the root-mean-square amplitude $\langle u^2\rangle^{1/2}$ is 0.076 Å for Si. This value has been deduced from x-ray data[6] and is calculated at a temperature of 301.7 K. Using Eqs. (10) and (9) in (3) and (7), the resulting values of σ' with thermal effects included are given in the last column of Table III, and although they are smaller than the experimental values, they agree within the experimental uncertainties.

The results demonstrate that planar channeling energy loss groups provide a very sensitive test of the form and size of the interplanar potentials, provided that the particles are totally stripped of electrons. Almost all of the data indicate that, as expected, different isotopes behave identically in planar channeling oscillations [i.e., $\nu_A(m_A)^{1/2} = \nu_B(m_B)^{1/2}$, where ν is the oscillation frequency and m the ion mass]. The data prove that the Molière potential, as it is commonly used, does not fit the correct form or size of the real interplanar potentials in silicon. In contrast, the Hartree-Fock potential provides an accurate fit to the data. The absence of any differences between He and Li indicate that, within the experimental errors, both nuclei behave as good test charges for the crystalline potentials in silicon.

TABLE III. Comparisons between the experimental and theoretical σ' factors.

Ion	σ(expt)[a]	σ'(theor)[b]	σ'(theor)[c]
He(110)	76.4 ±7	77.8	69.38
He(111)	66.8 ±6	78.3	62.94
Li(110)	91.7 ±6	95.2	85.0
Li(111)	83.0 ±5	95.9	77.10

[a]Experimental values extracted from the data of Table I using the relation $\sigma(\text{expt}) = \hat{s} - \alpha)\pi/\beta$, when the random stopping $\hat{s}$ is 7.25 ±0.07 eV/Å for He ions and 16.32 ±0.16 eV/Å for Li ions.
[b]Theoretical values without thermal corrections.
[c]Theoretical values with thermal effects included.

ACKNOWLEDGMENTS

The authors wish to acknowledge valuable discussion with M. T. Robinson on our modifications of his computer routines. This research is sponsored by the U.S. Department of Energy, Division of Basic Energy Sciences under Contract No. W-7405-ENG-26 with Union Carbide Corporation.

[1]S. Datz, C. D. Moak, T. S. Noggle, B. R. Appleton, and H. O. Lutz, Phys. Rev. 179, 315 (1969).
[2]M. T. Robinson, Phys. Rev. B 4, 1461 (1971).
[3]B. Sellers, F. A. Hanson, and J. G. Kelley, Phys. Rev. B 8, 98 (1973).
[4]C. C. Lu, T. A. Carlson, F. B. Malik, T. C. Tucker, and C. W. Nestor, Jr., At. Data 3, 1 (1971).
[5]F. H. Eisen and M. T. Robinson, Phys. Rev. B 4, 1457 (1971).
[6]B. W. Batterman and D. R. Chipman, Phys. Rev. 127, 690 (1962).